Memoirs of the Faculty of Engineering, Okayama University, Vol.38, Nos.1&2, pp.15-28, March 2004

Feature Extraction and Classification of Operational Data for Diagnosis of Hot Strip Mill Looper Control

Takashi Torigoe*
Division of Electronic and
Information System Engineering
Graduate School of Natural Science and Technology
Okayama University
3-1-1, Tsushima-Naka Okayama, 700-8530

Masami Konishi
Dept. of Electrical and Electronic Engineering
Okayama University
3-1-1, Tsushima-Naka Okayama, 700-8530

Jun Imai
Dept. of Electrical and Electronic Engineering
Okayama University
3-1-1, Tsushima-Naka Okayama, 700-8530

Tatsushi Nishi
Dept. of Electrical and Electronic Engineering
Okayama University
3-1-1, Tsushima-Naka Okayama, 700-8530

(Received February 13, 2004)

In these days, mechanical systems are becoming more complex and highly automated. So, there exist wide variety of demands for reliable diagnostic technology. A reliable data analysis and quantitative diagnosis method of mechanical system is necessary for the purpose. In this paper a quantitative diagnosis method for looper height control system has been developed based on neural network technologies. The wavelet transformation is used for pre-processing to analyze characteristics of looper height control system. And, self organizing map neural network is used for the purpose of classification based on the pre-processed data. After that, the classified results are used for quantitative diagnosis in hierarchical neural network.

1 Introduction

In these days, mechanical systems are becoming more complex and being highly automated, but on the other hand, there are still a lot of processes operation of which depends on a human especially failure diagnosis, parameter tuning, and so on. To realize quantitative diagnosis automatically, it is necessary to develop a new diagnostic technology. In this paper methods, analysis and classification of the operational data are studied to solve the problem.

Here, looper height control system in hot strip mills is focused as the target of failure diagnosis.[1] In hot strip mills, change in strip tension governed by the fluctuation of looper height during threading affects the quality of the product. So, it is needed to keep the control system in a high accuracy control level. However, there are difficulty to keep the quality at high level, because threading characteristics of strip rolling may not be stable. The change in characteristics may occur caused by deterioration or failure in one or more part of the system. From these reasons, it is needed to diganose cause of failure in hot strip mills to maintaining the products quality.

Diagnosis by human is flexible and generalized so that it is able to utilize not only in one particular conditions but also in other systems. The reason is that human can acquire the generalized knowledge of target system based on his or her experiences. Because of that, it is very difficult to replace the diagnosis by human with automatic system. The problem is quan-

*torigoe@cntr.elec.okayama-u.ac.jp

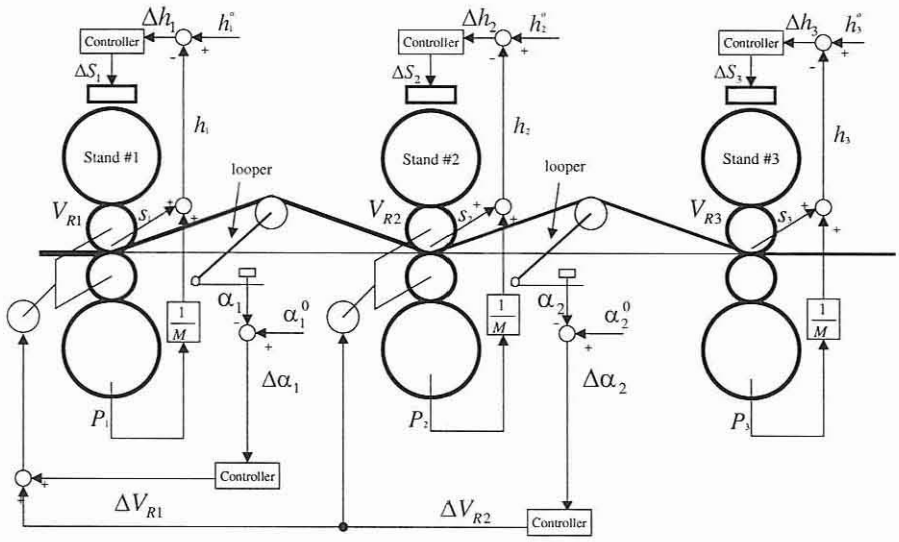

Fig. 1: Hot strip mill

titative diagnosis. Human can detect faults or defects intuitively but he or her can not diagnosis it quantitatively. In this paper, we try to approach quantitative diagnosis by the method of classification using self organizing map neural network. When human get data, it is compared with past data, and result of the comparison leads the conclusion. The purpose of this paper is to replace the procedure with the classification using SOM. Furthermore, possibility of reutilization of classified results to diagnosis is described.

2 The Looper control system in hot strip mills

Looper height control in hot strip mills is focused as a target system. In this section, looper height control system and its mathematical model are described. The structure of the hot strip mills is shown in Fig. 1.

2.1 The looper height control system

The looper height control system is used to keep the strip tension stable for an improvement of the product quality. The model for looper height control system consists of looper height model, strip thickness control and strip tension control. Factors which exerts an influence on the strip tension are described in the following.

2.1.1 The looper height model

The looper height is determined by difference of strip velocities between adjacent rolling stands. The variable and their geometrical relations between rolling stand #1 and #2 are shown in Fig. 2. The same relation can be stated for the situation between stand #2 and #3.

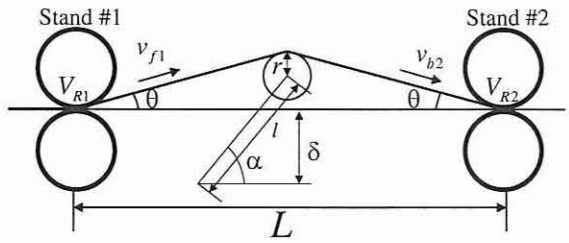

Fig. 2: Illustration of looper height control system between stand #1 and #2

The exit strip velocity v_{fi} and entry strip velocity v_{bi} of stand #i are written by

$$v_{fi} = V_{Ri}(1 + f_i) \tag{1}$$

$$v_{bi} = V_{Ri}(1 + \epsilon_i). \tag{2}$$

Where f_i is a forward slip ratio and ϵ_i is a backward slip ratio, These parameters are variables concerning the strip thickness control. And V_{Ri} is a rolling velocity.

The looper position is placed at the center of inter stands $(L/2)$ in Fig. 2. The strip loop angle θ is deter-

mined by the v_{f1} and v_{b2}.

$$\frac{1}{\cos\theta} = \frac{1}{L}\left\{L + \int_0^t (v_{f1} - v_{b2})\, dt\right\} \tag{3}$$

Where, $L + \int_0^t (v_{f1} - v_{b2})\, dt$ means the stand strip length between #1 and #2 stand. Then, looper height α is given by

$$\sin\alpha = \frac{1}{l}\left(\frac{L}{2}\tan\theta + \delta - r\right). \tag{4}$$

Where, the forward slip ratio f_i and the backword slip ratio ϵ_i are going to change when the strip thickness is controlled.

2.1.2 Mathematical model for hot rolling mills

The fundamental equations for rolling phenomenon are described as follows.

$$P = \sigma\sqrt{R'(H-h)}Q \tag{5}$$

$$Q = \sqrt{\frac{h}{H-h}}\left\{\frac{\pi}{2}\arctan\sqrt{\frac{H-h}{h}} - \sqrt{\frac{R'}{h}}\ln\frac{h_\phi}{h} + \frac{1}{2}\sqrt{\frac{R'}{h}}\ln\frac{H}{h}\right\} - \frac{\pi}{4} \tag{6}$$

$$h_\phi = \frac{h}{\cos^2 F} \tag{7}$$

$$F = \frac{1}{2}\arctan\sqrt{\frac{H-h}{h}} - \frac{\pi}{8}\sqrt{\frac{h}{R'}}\ln\frac{H}{h} \tag{8}$$

$$R' = R\left(1 + \frac{cp}{H-h}\right) \tag{9}$$

$$f = \frac{1}{2}\phi^2\left(\frac{2R'}{h} - 1\right) \tag{10}$$

$$\phi = \sqrt{\frac{h}{R'}}\tan F \tag{11}$$

$$\epsilon = \frac{h}{H}(1+f) - 1 \tag{12}$$

$$h = s + \frac{P}{M} \tag{13}$$

Where P is rolling force, σ is flow stress, H is entry strip thickness, h is exit strip thickness, R is roll radius, s is roll gap, f is forward slip ratio, ϵ is backward slip ratio, M is mill modulus. As described in Eq. (1) and Eq. (2), f and ϵ exerts an influence on the velocity of the strip. The exit strip thickness h is determined by roll gap s, mill modulus M and the entry strip thickness H using Eq. (5) to (13).

The control scheme of Gauge Meter AGC(Automatic Gauge Control) in stand #1 is shown in Fig. 3. The strip thickness control system controls the exit strip thickness at its aimed value h^o. AGC starts when the top end of strip enters into the next stand. The same thing is said for other stand.

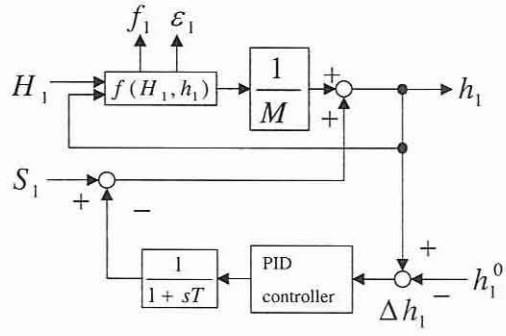

Fig. 3: The block diagram of the strip thickness control

2.1.3 The looper height control

The looper height control consists of looper height detection, PID controller and feedback operation. A block diagram of the looper height control system is shown in Fig. 4. $G(s)$ represents the relation of variables in Eq. (4).

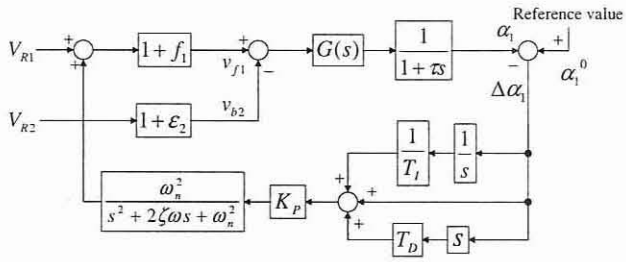

Fig. 4: Block diagram of looper height control system between stand #1 and #2

The figure shows that there is a 1st order time delay element after the output of $G(s)$. This time delay element is a representation of detection delay. After the detection of the looper height, V_{R1} is manipulated by PID control. There are 2nd order time delay element to manipulate V_{R1}, because of force transmission by torsion.

PID control is described as

$$m(t) = K_p\left(e(t) + \frac{1}{T_i}\int e(t)dt + T_d\frac{de(t)}{dt}\right) \tag{14}$$

where m(t) is manipulated variable V_{Ri} and e(t) is error meaning looper height deviation. K_p is proportional gain, T_i is integral time, and T_d is derivative time of PID control.

In simulator, PID control is used with velocity form algorithm.

$$V_{R1} = V_{R1} + \Delta V_{R1} \tag{15}$$

$$\Delta V_{R1} = K_p \left\{ (e_n - e_{n-1}) + \frac{T_s}{T_i} e_n + \frac{T_d}{T_s}(e_n - 2e_{n-1} + e_{n-2}) \right\} \tag{16}$$

Where T_s is sampling time interval, e_n is error at sampling time nT_s, e_{n-1} is error at sampling time $(n-1)T_s$, and e_{n-2} is error at sampling time $(n-2)T_s$

In order to decouple two loopers, rolling velocity at stand #1 and #2 formed as follows.

$$V_{R2} = V_{R2} + \Delta V_{R2} \tag{17}$$

$$V_{R1} = V_{R1} + \Delta V_{R1} + \Delta V_{R2} \frac{1+\epsilon_2}{1+f_1}. \tag{18}$$

2.1.4 The strip tension control

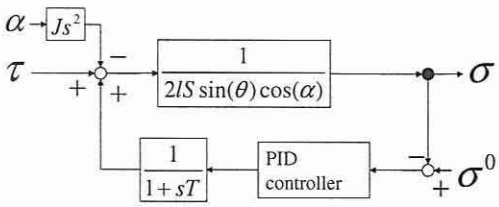

Fig. 5: Block diagram of tension controller

Using moment of inertia for looper J, looper length l, looper torque τ and looper height α, a force to the strip f generated by looper movement is written as follows.

$$J\ddot{\alpha} + fl = \tau \tag{19}$$

Then, the strip tension σ is written as

$$\sigma = f/(2lS\sin\theta\cos\alpha) \tag{20}$$

where, l, θ, α are same shown in Fig. 2, S is a cross sectional area of the strip. As shown in Fig. 5, τ is manipulated to control the strip tension σ.

Based on such relations, the block diagram for 3 stand hot strip mill with controller is shown in Fig. 6.

2.2 Looper height waveform

Here, the movement of looper height is simulated when the characteristics of looper height control system in the hot strip mills are changed.

In this paper, 4 factors are concerned as the characteristics which will be changed.

- proportional gain K_P of the PID controller in looper height control system
- aimed value α^o of the looper height
- time constant τ of the 1st order time delay element of the looper height sensing
- natural angular frequency ω_n of the 2st order time delay element of the rolling mill manipulation

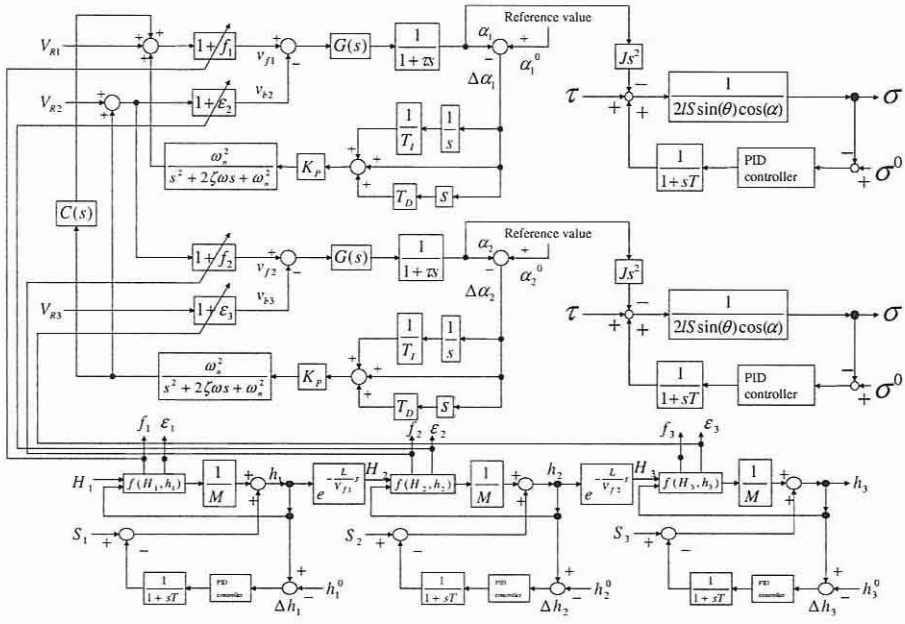

Fig. 6: Block diagram of 3 stand hot strip mill

The looper height is contolled by tuning the K_P and the α^o. The other two elements are internal values of the looper control system. Time delay τ of looper height sensing becomes large with the progression of deterioration in sensing euqipment. Natural angular frequency ω_n becomes small according to fatigue or deterioration in transmission system. These states are abnormal necessary to be found. Where, normal state means that time delay of the element is short time, and abnormal state means that time delay of the element is long time

The looper height waveforms when the K_P is changed are shown in Fig. 7 and Fig. 8. There is an overshoot when the K_P is large.

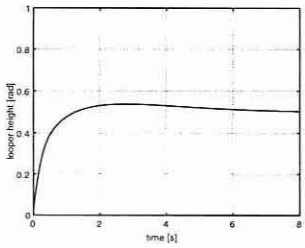

Fig. 7: normal state $K_P = 0.1$

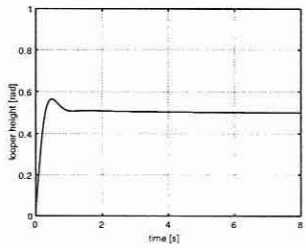

Fig. 8: normal state $K_P = 0.4$

The looper height waveforms when the K_P is changed when ω_n is small are shown in Figs. 9, 10. The small ω_n means time delay of manipulation is enlarged. So it becomes difficult to stabilize the looper height. The oscillation of looper height waveform is enlarged by change of ω_n in comparson with Fig. 8. However, By tuning the K_P, oscillation of the waveform is reduced. The same thing is stated for τ in Figs. 11, 12.

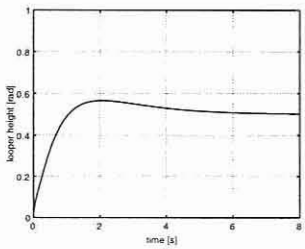

Fig. 9: small ω_n state $K_P = 0.1$

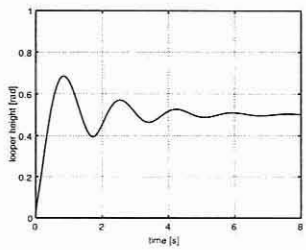

Fig. 10: small ω_n state $K_P = 0.4$

The looper height waveform when the aimed value α^o is changed are shown in Fig. 13 and Fig. 14. The conditions the looper height control system is same each other except the value α^o. Apparently from these figures, the aimed value α^o and proportional gain K_P of looper height controller greatly affect the performance of controlled results.

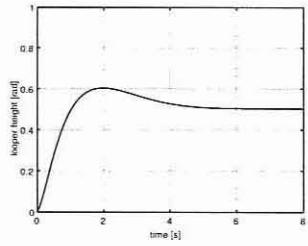

Fig. 11: large τ state $K_P = 0.1$

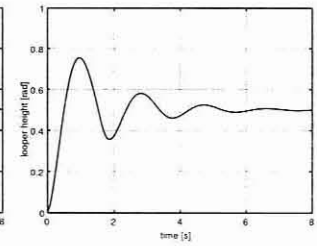

Fig. 12: large τ state $K_P = 0.4$

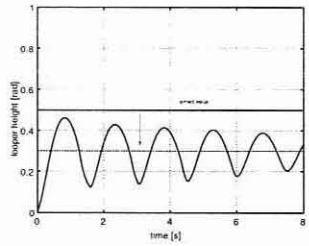

Fig. 13: $\alpha^o = 0.3$

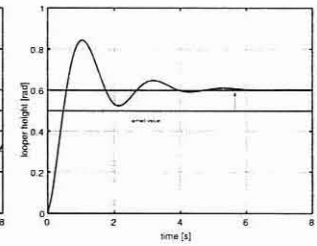

Fig. 14: $\alpha^o = 0.6$

3 Feature extraction

As described above, there may be little differences in observed wave data even if the values of parameters are entirely different. Therefore it is necessary to find new analysis method of input data to detect the difference between those waveforms. In this paper, time-frequency analysis by the wavelet transformation is applied to analyze the input data.

3.1 Wavelet transformation

There are many methods to execute time frequency analysis. The Fourier transformation is a very popular method to provide frequency analysis, although the time element is deleted from analyzed data. To solve this problem, short term Fourier transformation was developed. Wavelet transformation is another method solving its problem. Short term Fourier transformation is Fourier transformation for time-series data separated by window function. By separating analyzing data, it is able to analyze the data without losing the time element. The wavelet transformation method resembles short term Fourier transformation. Wavelet transformation does not separate the data, although it analyzes the data by analyzing wavelet without use of sine or cosine waves. Short term Fourier transformation modifies the data, and the data are analyzed by sine or cosine waves. Wavelet transformation analyzes the data by modified wavelet. A problem remains

in the short term Fourier transformation, When low frequency data is needed to be analyzed, the window function must be wide because it needs long time data. Conversely, when high frequency data is needed to be analyzed, only short time is needed. So, it needed the appropriate window function for frequency of the data to be analyzed.

Contrary to this, the wavelet transformation uses wavelet which can be modified. When low frequency data is analyzed, the wavelet must be wide function and vice versa.

The word "wavelet" means small wave. The input data is transformed in the fractional (mixed time frequency) domain by the wavelet.

The wavelet function which used in this paper is written in the following. Eq. (21) is multiplication of gauss function and cosine wave e^{-jt}.

$$\psi(t) = \frac{1}{2\sqrt{\pi}\sigma} e^{-\frac{t^2}{\sigma^2}} e^{-jt} \tag{21}$$

where, σ is set to 4 in this paper. The real part of Eq. (21) is shown in Fig. 15.

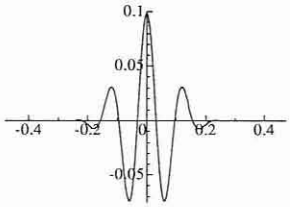

Fig. 15: Real part of $\psi(t)$

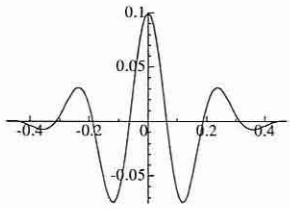

Fig. 16: Real part of $\psi\left(\frac{t}{2}\right)$

Using this wavlet $\psi(t)$, wavelet transformation of input signal $x(t)$ is defined as

$$(W_\psi f)(b,a) = \int_{-\infty}^{\infty} \frac{1}{\sqrt{a}} \overline{\psi\left(\frac{t-b}{a}\right)} x(t)dt \tag{22}$$

where, $(W_\psi f)(b,a)$ is a wavelet coefficient of the input signal $x(t)$ and $\psi\left(\frac{t-b}{a}\right)$ is analyzing wavelet. The a modifies the frequency of the analyzing wavelet. $\psi\left(\frac{t}{a}\right)$ is shown in Fig. 16. Fig. 16 is a waveform which is modified by a only in frequency domain. And b is a time shift in time domain.

By this equation (22), wavelet coefficient $(W_\psi f)(b,a)$ becomes larger when the input $x(t)$ is close to the analyzing wavelet determined by a, b.

The wavelet coefficient of example input $x(t) = 1 - cos(\omega(t)t)$ is shown in Fig. 17 making the $\omega(t)$ as kt.

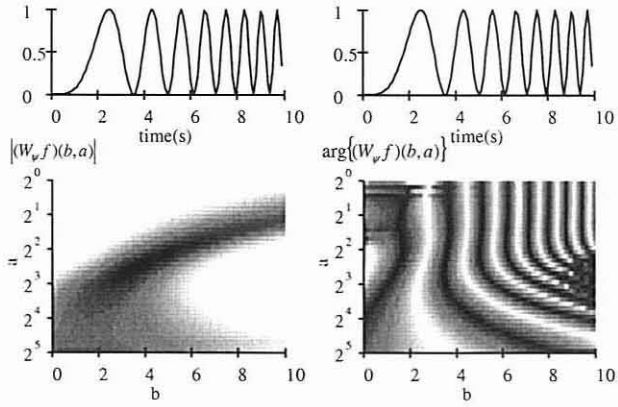

Fig. 17a: Absolute value Fig. 17b: Argument

Fig. 17: The wavelet coefficient of example input

The black areas on a, b-plane in Fig. 17a means that the magnitude of the wavelet coefficient at the position is large. Fig. 17a shows that there are correspondences at b to time and a frequency. The white areas in the Fig. 17b means that the phase lag between input and the wavelet is 0. Fig. 17b shows that many streaks in black and white appeared in the phase of the wavelet coefficient showing vibration of $x(t)$,not appeard in Fig. 17a. So, the wavelet analysis enables to separate the frequency and the vibration clearly.

3.2 Feature extraction by wavelet analysis

The example results of wavelet analysis applied to looper height waveform are described. An analyzed result is shown in Fig. 18, when the looper height waveform is normal in the looper height control sytem. As stated before, there are 2 types of time delay element in looper control system: 1st order time delay element and the other is 2nd order time delay element. The 1st order time delay element is characterized by τ, and in the case of the 2nd order time delay element is characterized by ω_n is the related parameter. In normal state these values are those of designed before hand. On the other hand, in abnormal state these values deviate from designed ones.

Fig. 18 shows that high frequency element exitsts at initial rise. While, Fig. 19 shows frequency is not so high at initial rize in comparison with Fig. 18. Although, it continues a little high frequency element widely in time domain.

Fig. 20 shows the analyzed result for the waveform related to abnormal τ value. And Fig. 21 shows one related to abnormal values of ω_n.

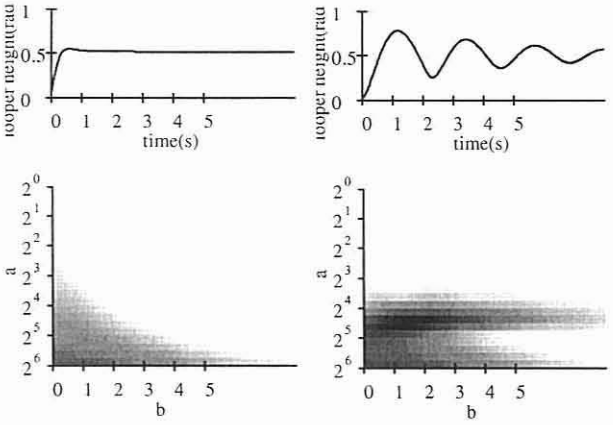

Fig. 18: normal state input

Fig. 19: τ and ω_n are failure

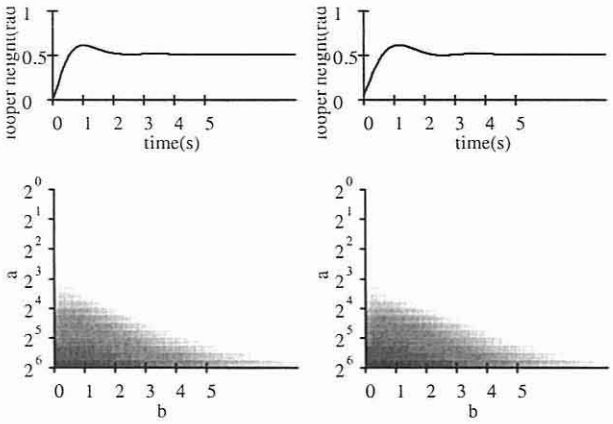

Fig. 20: Abnormal τ

Fig. 21: Abnormal ω_n

These figure show that there are little differences in absolute value of the analyzed data.

So, phase of the analyzed data are shown in Fig. 22 and Fig. 23.

As can be recognized in upper left side of these figures, there exist clear difference of black and white streaks between two waveforms. This means that there are differences in high frequency area at the initial rise.

4 Classification

As described above, the feature of the waveform is appeared to wavelet coefficients. The classification can be made using such coefficients. Human can find the feature of the wavelet coefficients and utilize them to diagnosis. When human get data, it is compared with past data, and result of the comparison leads the conclusion. However, it is difficult to execute those procedure automatically. In this section, the classification method by using SOM neural network is proposed.

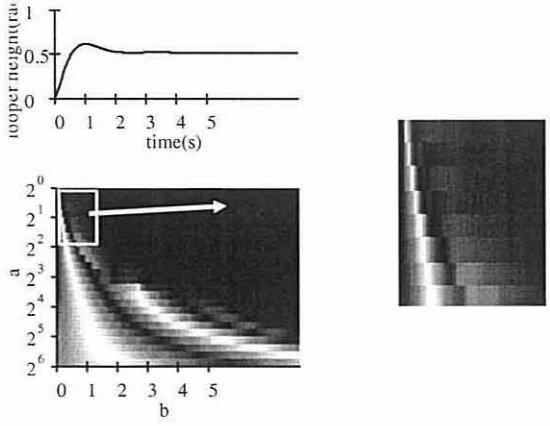

Fig. 22: the phase data when τ is abnormal

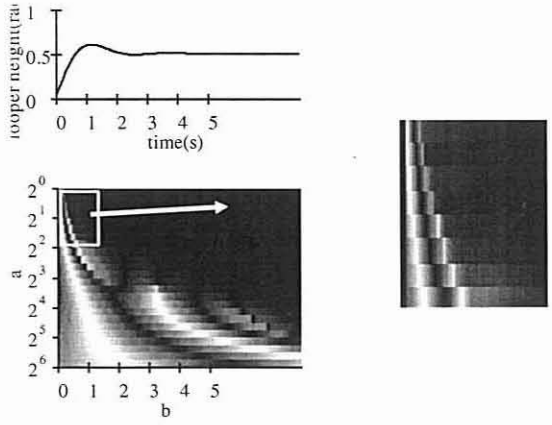

Fig. 23: the phase data when ω_n is abnormal

4.1 Self Organizing Maps(SOM) N. N.

SOM[3] is a multidimensional scaling method projecting input data space to lower dimentional output space. Typically, output data space is made as 2-dimension. Thus, input data space is visualized into 2-dimensional plane.

4.1.1 Structure of SOM N. N.

Self Organizing Maps(SOM) neural netwok consist of input layer and competitive layer. Input data is n-dimensional vector, and output data is 2-dimensional vector. Competitive layer has neurons organized in matrix. And accumulated information in each neuron is represented by weight vector. Dimension of the weight vector is equals to dimension of input data(n-dimension). Fig. 24 shows the structure of SOM.

The SOM is trained iteratively. In the training step, the input data vector x is input, and the distance between the data and all the weight vectors of the SOM is calculated. Where, Euclidean distance is used as

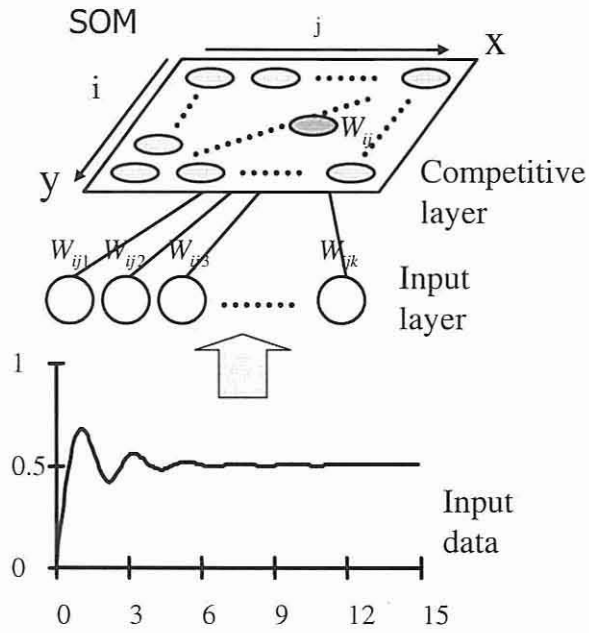

Fig. 24: Structure of SOM

distance measure in this paper. The neuron c whose weight vector is closest to the input vector x is chosen as the best-matching unit(BMU):

$$\|x - w_c\| = \min_{ij} \{\|x - w_{ij}\|\} \tag{23}$$

where, $\|.\|$ is the distance measure.

After finding the BMU, the weight vectors of the BMU is updated so that the weight of BMU is moved closer to the input data vector x. The neighbors of the BMU are also trained by a same way. The neighbors is defined by the distance from the BMU as follows,

$$r(t) = r_0 \left(1 - \frac{t}{T}\right) \tag{24}$$

where, t is time since the training started. T is the finising time of training. r_0 is initial range of neighbors.

The SOM update rule for the weight vector of the node (i, j) is written as

$$w_{ij}(t+1) = w_{ij}(t) + \alpha(t)\,[x(t) - w_{ij}(t)] \tag{25}$$

where, t is time, $x(t)$ is a input data vector x at time t. $\alpha(t)$ is a learning coefficient at time t, which is written as

$$\alpha(t) = \alpha_0 \left(1 - \frac{t}{T}\right) \tag{26}$$

where, α_0 is a initial learning coefficient. These parameters: α_0, r_0 and T is set to appropriate value, according to the problem.

After the above procedure is finished, the nodes of SOM whose weights are close to each other are gatherd in topologically restricted area. When certain input $x_{example}$ choses certain node $c_{example}$ as the BMU in the SOM, other input similar to $x_{example}$ choses a node nearby the $c_{example}$ as the BMU. In this paper, this feature of the SOM is used for the classification.

4.1.2 Condition of learnning

Here, the condition in the application of SOM for the classification of looper height waveforms. The looper height waveform is analyzed by wavelet transform, the feature of the waveform is emphasized to wavelet coefficient which is 2-dimentional matrix. The classification method by SOM is applied to the matrix data.

An illustration of the classification is shown in Fig. 25. SOM is trained by a lot of waveforms generated by looper control system in various cases.

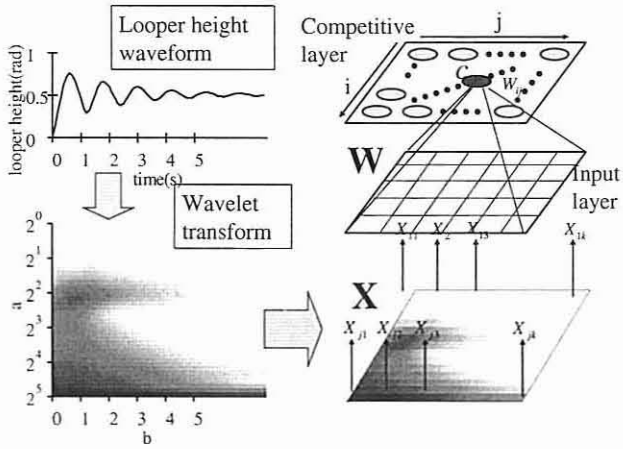

Fig. 25: construction of SOM analysis

Where the input waveforms are analyzed by using wavelet transformation as a pre-processing. The number of training times is set to 10000. The number of training data is 250. Where, sampling period is 0.05[s] and sampling time is 5[s]. The size of SOM N. N. in this case is 15×15.

4.2 Classified results

The nodes after training is visualized and shown in Fig. 26. This visualization is generated by u-matrix

method. The u-matrix is colored concerning the distance between adjacent nodes. Where the u-matrix is colored black if the distance is large.

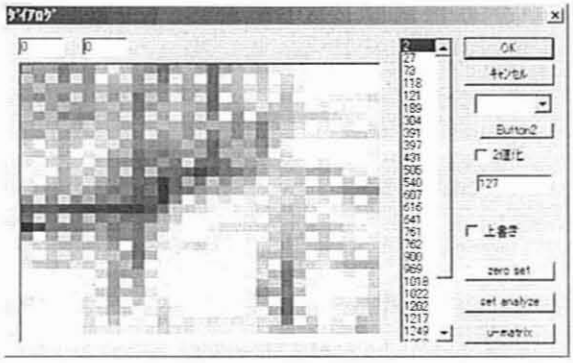

Fig. 26: u-matrix of classified result

Some extracted parts of classified results are shown in Fig. 39. These figure shows waveforms which are classified to each nodes. The figure of node(1,1) and node (1,8) show that stabilized waveform is collected in upper left nodes of the SOM. This means that waveform which generated by the looper height control system in normal state are collected in upper left of the SOM. Contrary to this, the figure of node(15,15) and node (15,8) show that oscillating waveform is collected in lower right of the SOM. This means that waveform which generated by the looper height control system in abnormal state are collected in lower right of the SOM. And the others of the nodes collects waveforms which resembles each other. using this method difference between waveforms can be recognized even if human can not recognize it.

Next, the classified ratio of each nodes in the SOM is described. Next, parameter values τ and ω_n are analyzed. The failure is considered at small ω_n value and at large τ value. In this case, for failure conditions, $\omega_n < 13$ and $\tau > 0.25$ are considered. Table 1 shows 4 cases of τ and ω_n conditions.

Table 1: The cases of τ and ω_n conditions

	τ normal $\tau \leq 0.25$	τ abnormal $\tau > 0.25$
ω_n abnormal $\omega_n \leq 13$	case 1	case 2
ω_n normal $\omega_n > 13$	case 3	case 4

Fig. 27 shows classified results for data of case 1. Lines in Fig. 27 are contour lines corresponding to the ratios whith which the data is recognized as case 1. These analyzed results are shown in Figs. 28 to 30 respectively.

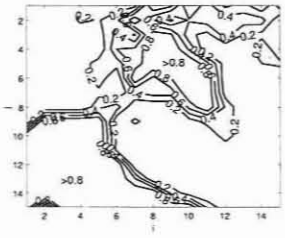

Fig. 27: case 1

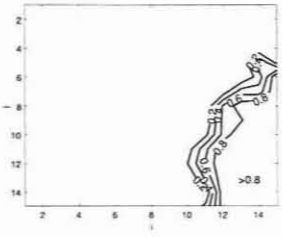

Fig. 28: case 2

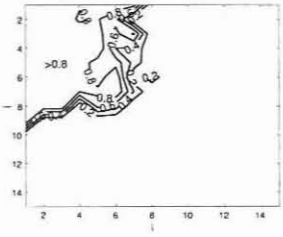

Fig. 29: case 3

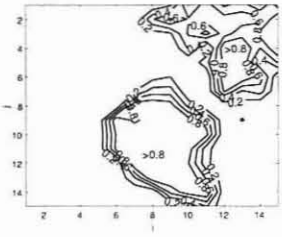

Fig. 30: case 4

Fig. 39 is applied this result, a state of the classified waveform in each nodes is roughly defined as below. The node(1,15) and node(8,1) are related to case 1. The node(15,8) and node(15,15) are related to case 2. The node(1,1) and node(1,8) are related to case 3. The node(15,1) and node(15,8) are related to case 4.

By classifying the wave form, the data is projected to the 2-dimensional plane. From the position of the plane, it is possible that diagnosis of waveform viora-tion or estimation of failure causes.

5 Diagnosis using classified data

In this section, quantitative diagnostic method is described. For the purpose, hierarchical neural network model is introduced to estimate control parameters in looper height controller.

5.1 Estimation of system parameters

The diagram of estimation process that we propose is shown in Fig. 31.

First, the looper height waveform is analyzed by the SOM and wavelet transformation. The classified results and the looper height waveform is input into the hierarchical neural network. Then, the network learns the correlation of the input and according to the parameters in the looper height control system, which

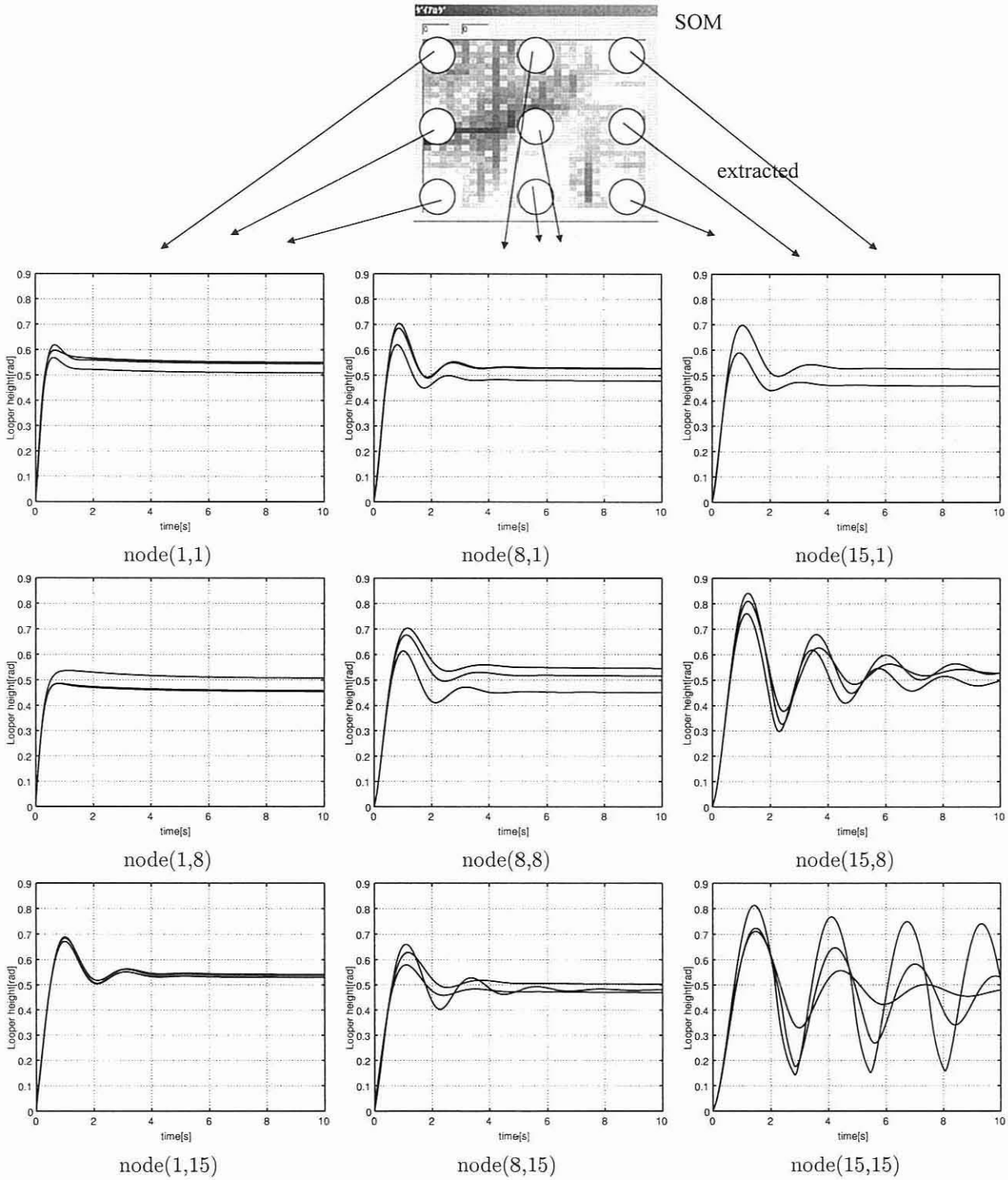

Fig. 39: Classified result

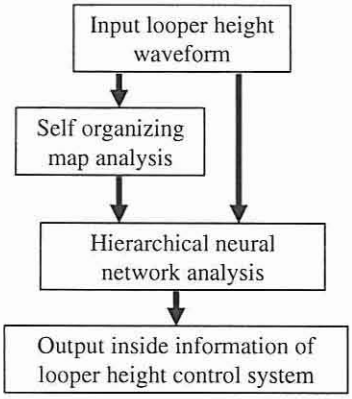

Fig. 31: Diagram of diagnosis using neural networks

provides the fault of the system. Finally, the network estimate parameters in the system according to input data. As for the parameters, time constant τ of the 1st order time delay element,natural angular frequency ω_n of the 2st order time delay element and proportional gain K_P of the PID controller are diagnosed.

5.2 Hierarchical neural network

Neural network is a simplified model of the human brain. It consists of one or more artificial neurons. Therefore, it has the ability to learn and adapt. Also, there are many industrial applications. The hierarchical neural network (HNN) is one of artificial neural networks.[2, 4] The structure of the HNN is shown in Fig. 32.

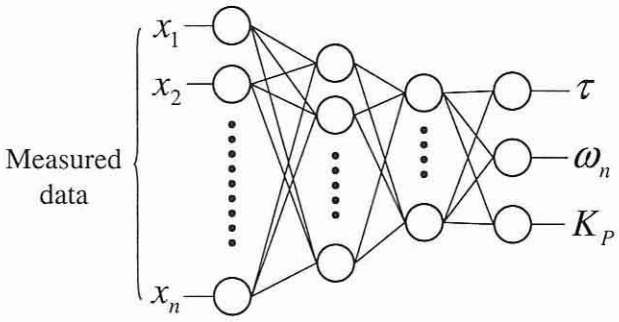

Fig. 32: Structure of neural network

As shown in Fig. 32, the HNN consists of multiple layers. Each layer has multiple artificial neurons. It means that artificial neurons are hierarchically combined in the HNN. The combined neurons make it possible to execute non-linear mapping from input to output.

In this paper, the input of HNN is data which contains looper height waveform and classified results. And the output of HNN is the parameters in the looper height control system, which provides the fault of the system. The input of Fig. 32 don't include the classfied results. Structure of the HNN with the classified results is shown in Fig. 33.

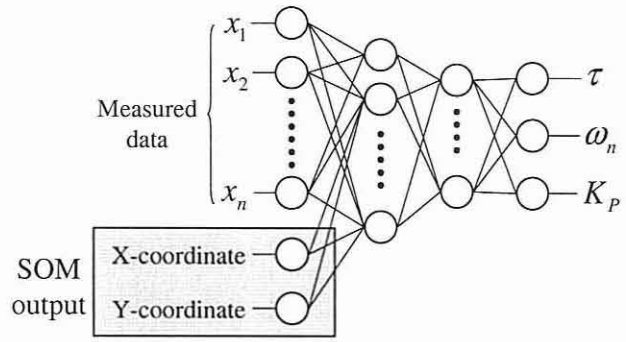

Fig. 33: Structure of neural network using classified data

The HNN model with the classified results and HNN model without classified results are trained and compared. These models are trained 5000 times using 500 looper height waveform data which is ramdomly generated. After the training is finished, another 1500 waveform data is applied to these models.

As described above, In this paper, 4 factors are concerned as the characteristics which will be changed.

- proportional gain K_P of the PID controller in looper height control system
- aimed value α^o of the looper height
- time constant τ of the 1st order time delay element of the looper height sensing
- natural angular frequency ω_n of the 2st order time delay element of the rolling mill manipulation

α^o and K_P is a configurable parameters by human. Although, parameters to be estimated is τ, ω_n and K_P concerning tuning mistake.

5.3 Estimated results

Schematic diagram of the estimation system is shown in Fig. 34. This figure shows result of the estimation described above. Input waveform data in Fig. 34 are changed depending on the changing parameters τ, ω_n

and K_P. These waveforms are input to the estimation system. Parameters τ, ω_n and K_P are estimated by the estimation system in response to these changing waveforms. As is shown here, changes in parameters τ, ω_n and K_P are estimated and being output from the network. As shown in Fig. 34, the estimated parameters are in good coincidence with those of actual. Thus, the function of the diagnostic system could be ascertained.

Other Results of the estimation are shown in Figs. 35, 36. The horizontal axis in these figures is actual parameters of looper height control system, And the vertical axis indicates the estimated parameters. If parameters are estimated with no error, dotted points in these figures are on a straight line.

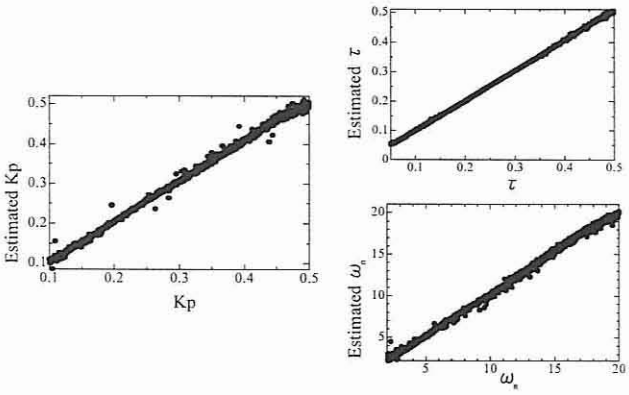

Fig. 35: charasteristics estimation with SOM

Figs. 35, 36 shows that result of estimation using SOM are more accurate. This means that the estimation error is reduced by using SOM.

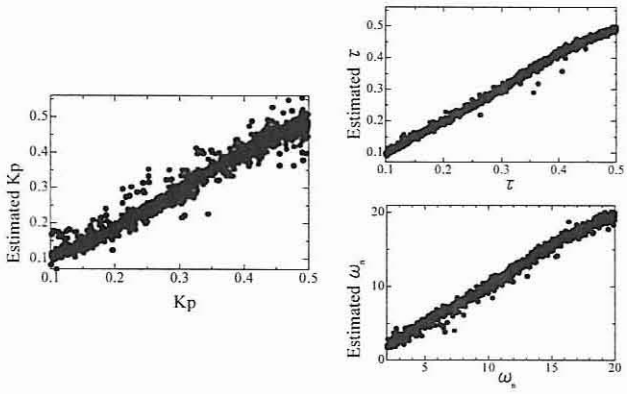

Fig. 36: charasteristics estimation without SOM

Standard deviation σ of the estimation error is shown in Table 2. σ is defined by Eq. (27)

$$\sigma = \sqrt{\frac{\Sigma_{i=1}^{n}(e_i - \bar{e})^2}{n-1}} \tag{27}$$

where, e is error between actual value and estimated value. Table 2 shows that the estimation error of the model without using SOM is more than twice larger as the estimation error using SOM.

Table 2: Standard deviation of the estimation error

	σ_τ	σ_{ω_n}	σ_{K_P}
with SOM	0.003	0.24	0.005
without SOM	0.009	0.48	0.012

An example of estimated data by N. N. is shown in Fig. 37 by using HNN without classified results. And

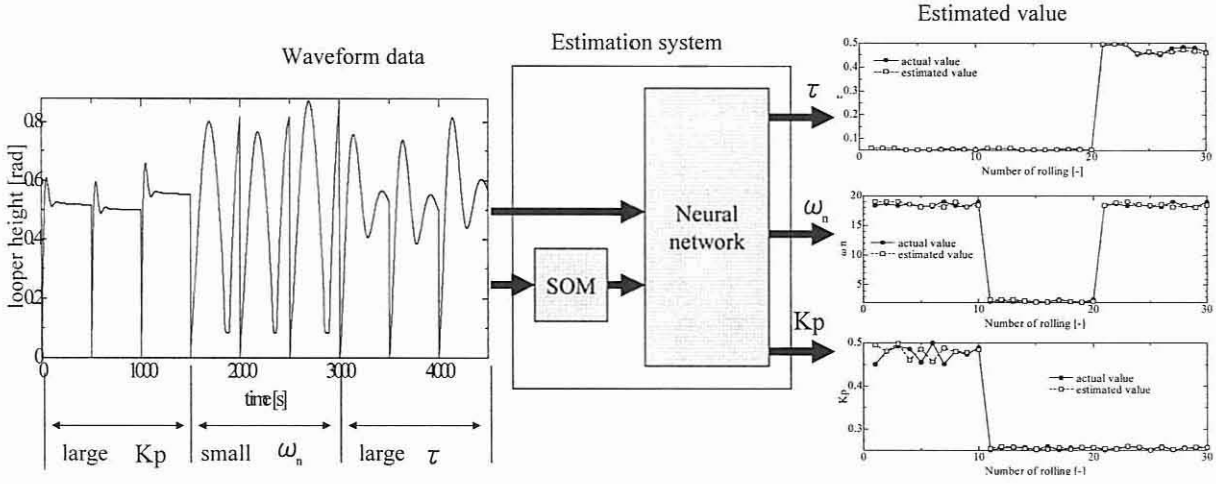

Fig. 34: schematic diagram of estimation with SOM

Fig. 38 is the result when the same data is input to the HNN in Fig. 33 with classified results.

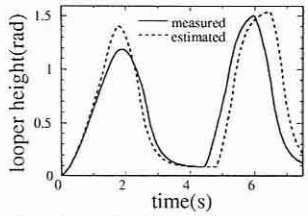

Fig. 37: Estimated waveform without SOM

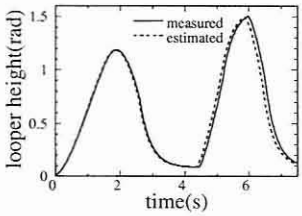

Fig. 38: Estimated waveform with SOM

These figures, it is known that the result of classification by the SOM improve the accuracy of estimation. This is because there exist a tendency of the actual parameter depending on the positon of the SOM. As shown in this figure, the accuracy of estimation could be improved by the information of the position.

6 Conclusion

In this paper, classification using SOM neural network for quantitative diagnosis in system diagnosis is introduced. Wavelet analysis makes the feature of waveform at failure state in looper height control system appear on 2-dimension matrix. It is realized that failure or mistake of looper height control is detected by classification using SOM neural network. Using the model, accurate quantitative estimation of parameters ω_n and K_P in looper controller can be made.

In running system, there are difficulties to get data for estimation. The system we probpose only needs waveform data to estimate. So, application of the system to on-line estimation of running system is expected.

Bibliography

[1] H.Asada et al, "Adaptive and Robust Control Method with Estimation of Rolling Characteristics for Looper Angle Control at Hot Strip Mill", ISIJ International, Vol.43, No.3(2003), pp358-365

[2] I.M.Mujtaba et al, "Application of Neural Networks and Other Learning Technologies in Process Engineering", Imperial College Press, 2001

[3] Lakhmi C.Jain et al, "INDUSTRIAL APPLICATIONS of NEURAL NETWORKS", The CRC Press, 1999

[4] Cihan H. Dagli, "ARTIFICIAL NEURAL NETWORKS for Intelligent Manufacturing", Chapman & Hall, 1994

[5] S.Imajo et al, "Human Model and its Learning for Setting of Looper Control Gain in Threading of Hot Tandem Mills," Proc. of the 46th Annual Conf. of the Institute of Systems, Control and Information Engineers (2002), pp.521-522

[6] S.Imajo et al, "Human Model for Gain Tuning of Looper Control in Hot Strip Rolling," CAMP-ISIJ, Vol.15(2002), p931